Catal Lett (2008) 126:10–19
DOI 10.1007/s10562-008-9637-8

Influence of Particle Size on Reaction Selectivity in Cyclohexene Hydrogenation and Dehydrogenation over Silica-Supported Monodisperse Pt Particles

R. M. Rioux · B. B. Hsu · M. E. Grass · H. Song · G. A. Somorjai

Received: 11 June 2008 / Accepted: 2 September 2008 / Published online: 11 October 2008

Abstract The role of particle size during the hydrogenation/dehydrogenation of cyclohexene (10 Torr C_6H_{10}, 200–600 Torr H_2, and 273–650 K) was studied over a series of monodisperse Pt/SBA-15 catalysts. The conversion of cyclohexene in the presence of excess H_2 (H_2:C_6H_{10} ratio = 20:60) is characterized by three regimes: hydrogenation of cyclohexene to cyclohexane at low temperature (<423 K), an intermediate temperature range in which both hydrogenation and dehydrogenation occur; and a high temperature regime in which the dehydrogenation of cyclohexene dominates (>573 K). The rate of both reactions demonstrated maxima with temperature, regardless of Pt particle size. For the hydrogenation of cyclohexene, a non-Arrhenius temperature dependence (apparent *negative* activation energy) was observed. Hydrogenation is structure *insensitive* at low temperatures, and apparently structure *sensitive* in the non-Arrhenius regime; the origin of the particle-size dependent reactivity with temperature is attributed to a change in the coverage of reactive hydrogen. Small particles were more active for dehydrogenation and had lower apparent activation energies than large particles. The selectivity can be controlled by changing the particle size, which is attributed to the structure sensitivity of *both* reactions in the temperature regime where hydrogenation and dehydrogenation are catalyzed simultaneously.

Keywords Cyclohexene · Hydrogenation · Dehydrogenation · Platinum · Particle size · Selectivity

1 Introduction

Considerable work has been conducted to demonstrate the effect of particle size on reaction activity [1]. Reactions whose rate varies with particle size are referred to as structure sensitive and those independent of particle size are termed structure insensitive [2]. The effect is often seen in the particle size range of 1–5 nm, the region over which the fraction of surface sites with different coordination change most drastically. At particle sizes above 5 nm, bulk crystal habits have developed and changes in particle size lead to little change in the average coordination number. Experimentally, the apparent sensitivity of a reaction to the structure of a catalyst is determined by measuring the rate of reaction over a series of catalysts with varying particle size (ideally with catalysts who particle size is monodisperse [3, 4]). To this end, we synthesized nearly monodisperse Pt nanoparticles (NPs) (1.7–7.1 nm) by solution-phase colloidal methods, incorporated them into mesoporous SBA-15 silica matrices and constructed structure (particle size)–activity relationships for the *one* product reactions, ethylene hydrogenation and ethane

R. M. Rioux · B. B. Hsu · M. E. Grass · H. Song ·
G. A. Somorjai (✉)
Department of Chemistry, Berkeley and Lawrence Berkeley
National Laboratory, Materials and Chemical Sciences Division,
University of California, Berkeley, CA 94720, USA
e-mail: somorjai@berkeley.edu

Present Address:
R. M. Rioux
Department of Chemical Engineering, Pennsylvania State
University, University Park, PA 16802, USA

B. B. Hsu
Department of Chemistry, Massachusetts Institute of
Technology, Cambridge, MA 02139, USA

H. Song
Department of Chemistry and School of Molecular Science
(BK21), Korea Advanced Institute of Science and Technology,
Daejeon 305-701, South Korea

hydrogenolysis [3, 4]. In this manuscript, we utilize the same set of monodisperse Pt NPs supported on SBA-15 catalysts to correlate the *influence of particle size on selectivity* during the hydrogenation–dehydrogenation of cyclohexene.

The hydrogenation of cyclohexene to cyclohexane on supported nanoparticle catalysts at ambient temperature[1] is structure insensitive [5], similar to benzene hydrogenation on supported Pt catalysts [6]. The measurement of the rate of cyclohexene hydrogenation on Pt single crystals under high pressure conditions and *ambient* temperature confirms the structure insensitivity of the reaction [7, 8].

The dehydrogenation of cyclohexene to benzene is structure sensitive on close-packed Pt single crystal surfaces; dehydrogenation proceeds more rapidly on the Pt(100) crystal surface than on the Pt(111) crystal surface [7, 8]. Two reaction intermediates have been observed spectroscopically on both single crystal surfaces. On Pt(100), 1,3-cyclohexadiene (CHD) is observed, whereas on Pt(111), both the 1,3- and 1,4-CHD species dehydrogenate to form benzene. The structure sensitivity of cyclohexene dehydrogenation is explained by noting that there is both a fast and slow reaction pathway on Pt(111); the slow 1,4-CHD pathway effectively eliminates surface sites for the faster 1,3-CHD pathway to turnover. The only pathway present on Pt(100) is through 1,3-CHD, where all active sites on Pt(100) participate in the fast reaction pathway [8].

Both hydrogenation and dehydrogenation products (cyclohexane and benzene) are thermodynamically-allowed and formed over Pt catalysts at intermediate temperatures ($400 \leq T \leq 600$ K). Previous work on silica-supported Pt catalysts demonstrated cyclohexene and benzene are not formed with thermodynamic selectivity [9]. There has been little examination of the influence of surface structure (or particle size) on the *selectivity* of cyclohexene conversion in excess hydrogen over experimental conditions where the formation of both cyclohexane and benzene is thermodynamically permissible [9] because most experimental studies have focused on conditions where only hydrogenation occurs (low temperature) or conditions where only dehydrogenation [5, 10] occurs (high temperature) [11, 12].

Little is known about the *structure sensitivity of reaction selectivity* [13]. Selectivity can be altered by eliminating certain types of sites from the surface of NPs. A convincing demonstration of the role of specific surface sites controlling selectivity in a catalytic reaction was demonstrated recently for the chemoselective hydrogenation of acrolein over supported gold nanoparticle catalysts [14, 15]. For Au nanoparticle catalyzed acrolein hydrogenation, the *edges* of single-crystalline gold particles have been identified as the active sites for the preferred C=O hydrogenation suggesting that the size (and/or shape) of the nanoparticle can influence reaction selectivity [15]. The activity (and therefore selectivity) to the unsaturated alcohol during the chemoselective hydrogenation of crotonaldehyde increased with increasing particle size [16].

Our previous approach to understand the influence of particle size on catalytic activity has been to synthesize transition metal nanoparticle SBA-15-supported catalysts in which the particle size is carefully controlled by solution-phase nanoparticle synthesis [3, 4, 17]. In this paper, we examine the effect of particle size on reaction selectivity for the conversion of cyclohexene in excess hydrogen. We demonstrate that in a regime where both cyclohexene and benzene form, the surface is depleted in hydrogen and the particle size influences reaction selectivity through a particle size dependent reactive hydrogen coverage.[2] The hydrogenation of cyclohexene is structure insensitive under conditions of reversible hydrogen adsorption (low temperature) and becomes structure sensitive with an apparent dependence on hydrogen pressure which is much greater than unity at higher temperatures. We compare our results with kinetic measurements on platinum single crystals, which confirm the structure sensitivity of *selectivity* in cyclohexene hydrogenation–dehydrogenation in excess hydrogen [8].

2 Experimental

2.1 Catalyst Synthesis and Characterization

A series of ~0.6% Pt(*X*)/SBA-15 ($X = 1.7$, 2.9, 3.6, and 7.1 nm) catalysts were used in these experiments. A detailed description of their synthesis and characterization has been published previously [3, 4]. Pt NPs between 1.7 and 7.1 nm protected by polyvinylpyrrolidone (PVP) are synthesized by modified alcohol reduction methods to yield nearly monodisperse Pt NPs. After synthesis of the NPs, we

---

[1] The hydrogenation of cyclohexene at low temperatures is thermodynamically preferred, while dehydrogenation dominates at high temperature, and the switch between preferential hydrogenation and dehydrogenation occurs over a very narrow temperature range. Reaction temperatures of 400 K favor hydrogenation ($K_h/K_d = 10^7$), while 600 K favors dehydrogenation ($K_h/K_d = 10^{-2}$).

[2] The influence of particle size on the coverage of hydrogen is complicated due to the presence of multiple hydrogen species on a Pt surface as demonstrated in temperature-programed desorption (TPD) studies. If only a single population of adsorbed hydrogen is present on the surface, the effect is simply one of low surface coverage. However, if there are various populations of adsorbed hydrogen on the surface of the nanoparticle, the particle size dependence may be a result of the inability of one particle size to support a particular population (sub-species) of adsorbed hydrogen under reaction conditions.

encapsulated them in a SBA-15-like structure by direct participation in the hydrothermal process for mesoporous silica formation. The synthesis of SBA-15 is conducted at neutral pH using NaF as a catalyst for hydrolysis of the silica precursor [18], conditions which differ from the original description of SBA-15 synthesis [4]. Catalysts are activated ex situ prior to catalysis by calcination in 20% O_2/He (or pure O_2) and reduced in situ directly before reaction in order to remove PVP fragments and adsorbed oxygen from the surface of the particle [4]. A 3.2% Pt/SiO_2 catalyst prepared by ion-exchange of $Pt(NH_3)_4(OH)_2 \cdot xH_2O$ at pH 9 [19] was used as a standard sample for reaction studies. We reduced this catalyst [herein referred to as Pt(1 nm)/SiO_2] by an identical in situ procedure used for the SBA-15 catalysts.

The characterization of these catalysts has been published previously [3, 4, 20]. The particle size determined by selective chemisorption (H_2–O_2 titration) differed from the as-synthesized size measured for the unsupported clusters by X-ray diffraction and transmission electron microscopy [3], which we believe is primarily due to the influence of residual PVP on the surface of the nanoparticle.

Kinetic measurements were conducted in a plug-flow reactor (PFR) operating under differential conditions (conversion varied between 1 and 20%). Calcined Pt/SBA-15 catalysts (2–5 mg) diluted in acid-washed low surface area quartz (10–25 mg) were reduced in situ (directly in the PFR) prior to reaction. Helium and H_2 were delivered to the reactor with mass flow controllers (Unit Instruments Corporation, Model UFC 1200) while cyclohexene was pumped (typical volumetric flow rates were 1–10 mL h^{-1}) into the He/H_2 flow by a syringe pump (Cole Parmer). All lines before and after the quartz U-tube reactor were heated to 393 K to prevent condensation of organic compounds. After allowing the catalyst to reach a steady-state activity at 273 or 298 K, the catalyst bed was heated in ascending order (20 K increments) and cooled (first by 10 K, and then in 20 K increments) back to room temperature. There was no hysteresis in the temperature-dependent activity data suggesting that irreversible deactivation at high temperature was minimal. Reactant and product concentrations were measured during the ascending and descending temperature sequence with a gas chromatograph (Hewlett Packard 5890 Series II) equipped with a ten way-sampling valve allowing simultaneous monitoring of organics with a flame ionization detector (FID) and thermal conductivity detector (TCD) for detection of hydrogen. The mass activity (μmol g^{-1} s^{-1}) for both cyclohexane and benzene were calculated from the measured chromatograph peak area using response factors [21] and assuming a rate equation for a differential reactor. The turnover frequency (TOF) for both products was calculated by normalizing the mass activity (μmol g^{-1} catalyst s^{-1}) to the number of surface Pt atoms (Pt_s) determined by H_2–O_2 titration [3, 4].

3 Results and Discussion

3.1 Influence of Temperature on Cyclohexene Hydrogenation–Dehydrogenation

The temperature dependence of cyclohexene hydrogenation–dehydrogenation can be divided into three regimes (hydrogenation only, hydrogenation + dehydrogenation, and predominantly dehydrogenation) [22]. Hydrogenation is the only reaction at low temperatures ($\leq$400 K), while simultaneous hydrogenation and dehydrogenation occurs from ~400 to 600 K at standard conditions (10 Torr C_6H_{10}, 200 Torr H_2, balance He). Dehydrogenation is the dominant reaction path at temperatures $\geq$600 K. Figure 1 demonstrates that within the three regimes, the hydrogenation rate follows normal temperature dependent (Arrhenius) behavior, goes through a well-defined maximum (~350 K) and then decreases with increasing temperature. The third regime is commonly referred to as 'non-Arrhenius' or 'bend-over' behavior [23] and has been reported for the hydrogenation of benzene on carbon-supported Fe and Pt catalysts [24, 25], the reforming of hexane in excess hydrogen on Pt catalysts [23, 26, 27], alkane hydrogenolysis [28, 29] and cyclohexene hydrogenation on a Pt(111) and Pt(100) single crystal surfaces [8, 30, 31]. In the third regime ($T > 600$ K), the production of cyclohexane has decreased considerable (with turnover rates (~3 s^{-1}) comparable to those measured at 300 K). The rate of dehydrogenation begins to decrease which is probably related to a decrease in cyclohexene and/or H_2 coverage. Decreased activity at higher temperatures in not attributed to the deposition of carbon because during the decreasing temperature ramp, the measured rates fall in between the activity points measured during the ascending temperature ramp.

This non-Arrhenius behavior for the hydrogenation of cyclohexene leads to a negative *apparent* activation energy and is commonly associated with unfavorable adsorption thermodynamics leading to a low coverage of either C_6H_{10} or H_2, respectively. Yoon and Vannice noted a maximum TOF at ~473 K for C_6H_6 pressures (20–100 Torr), which decreased to ~453 K at lower pressures (<3 Torr) for C_6H_6 hydrogenation of over a supported-Fe catalyst. The increased benzene partial pressure affords a larger coverage of benzene. Yang and co-workers suggested recently that the 'bend-over' Arrhenius behavior for cyclohexene hydrogenation on Pt(111) was due to a low cyclohexene coverage [30]. Low hydrogen coverage has been proposed

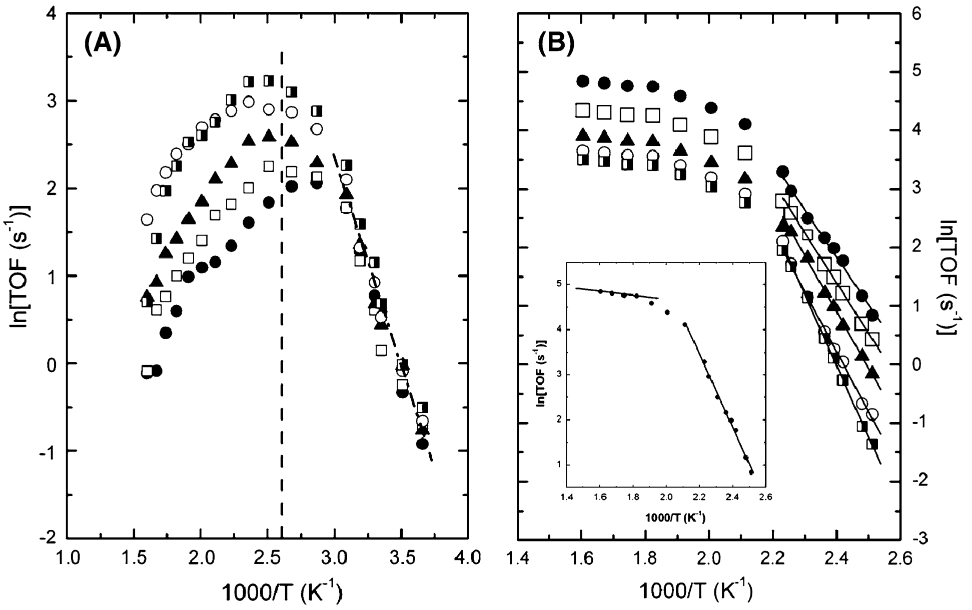

Fig. 1 Arrhenius plots for cyclohexene (**a**) hydrogenation and (**b**) dehydrogenation on (●) 3.2% Pt(1 nm)/SiO_2; (□) 0.6% Pt(1.7 nm)/SBA-15; (▲) 0.77% Pt/(2.9 nm)/SBA-15; (○) 0.6% Pt(3.6 nm)/SBA-15; and (◨) 0.62% Pt(7.1 nm)/SBA-15. The Arrhenius plots for hydrogenation undergo a change in the sign of the slope (non-Arrhenius behavior) at a temperature of ~350 K for all particle sizes. The Arrhenius plot for dehydrogenation demonstrates the rate begins to level off at a temperature of ~550 K. The inset of (**b**) shows that the slope at high temperature corresponds to an apparent activation energy (E_{app}) of ~2 kcal mol^{-1}, while the low temperature E_{app} (Arrhenius regime) is an order of magnitude larger for the 3.2% Pt(1 nm)/SiO_2 catalyst. The rates were measured at 10 Torr C_6H_{10}, 200 Torr H_2 and balance He. The dashed vertical line in (**a**) represents the temperature at which dehydrogenation activity is measured initially

by others as the cause for non-Arrhenius behavior during hydrogenation reactions. Paál measured a maximum rate for hydrocarbon reforming reactions, and demonstrated it is related to a hydrogen coverage effect [23]. As the reaction temperature increases at constant hydrogen pressure, the hydrogen coverage and the rate of hydrocarbon reforming decreases. Paál suggested that measuring the rate maxima—where the dependence on H_2 is zero order—as function of reaction temperature should yield a 'normal' apparent activation energy [23]. We examine the influence of hydrogen partial pressure on the non-Arrhenius behavior in Sect. 3.4.

3.2 Temperature Dependent Structure Sensitivity of Cyclohexene Hydrogenation–Dehydrogenation

The activity, TOF, and apparent activation energy for both the hydrogenation and dehydrogenation of cyclohexene are compiled in Table 1. The rates for both reactions measured on a Pt(111) and Pt(100) single crystal are also included in Table 1 [8]. The hydrogenation TOF at 313 K is structure insensitive, the rates are ~3.5 s^{-1} and the apparent activation energy is ~9 kcal mol^{-1}. Cyclohexene hydrogenation is structure sensitive at low temperature, but as the temperature is increased into the 'non-Arrhenius' regime, the reaction becomes structure sensitive. Figure 2 demonstrates at 448 K, the TOF on Pt(7.1 nm)/SBA-15 is a factor of four greater than the TOF on Pt(1.7 nm)/SBA-15. This difference is proposed to be due to a particle-size dependence on the total H_2 coverage (i.e., a bare surface) or a decreased coverage of a particular population (sub-species) of adsorbed hydrogen (weak, moderately or strongly adsorbed hydrogen). We explore both of these scenarios by examination of published data on the measured differential heat of hydrogen adsorption [$\Delta H_{ads}(\theta = 0)$ dependence] and TPD behavior of silica-supported Pt catalysts. Vannice and co-workers demonstrated there is no dependence of the initial heat of adsorption of H_2 on the Pt particle size on SiO_2-supported catalysts [32]; even though the heat of adsorption of hydrogen on single crystal surfaces is facet-dependent [33, 34]. Based on the significant scatter in reported values for the integral (and differential) heats of adsorption of H_2 at room temperature on silica-supported Pt catalysts, we propose that the heat of adsorption of a particular population of adsorbed hydrogen is particle-size dependent and represents the reactive hydrogen in the hydrogenation/dehydrogenation of cyclohexene. TPD of adsorbed hydrogen from SiO_2-supported Pt NPs demonstrate that there can be up to three different populations of adsorbed hydrogen with desorption temperatures centered at ~370, 600 and 740 K [35]. The maximum temperature of desorption for

Table 1 The activity and selectivity for cyclohexene hydrogenation–dehydrogenation and the apparent activation energy (in the linear regime) over SiO_2-supported Pt catalysts

Catalyst[a]	Particle size by chemisorption (nm)[b]	Hydrogenation			Dehydrogenation		
		Activity[c] (μmol g^{-1} s^{-1})	TOF[d] (s^{-1})	E_a[e] (kcal mol^{-1})	Activity[c] (μmol g^{-1} s^{-1})	TOF[d] (s^{-1})	E_a[f] (kcal mol^{-1})
3.2% Pt/SiO_2	1	590	3.6	9.6	1427	8.7	16.0
0.6% Pt(1.7 nm)/SBA-15	2.7	41	3.2	8.7	71	5.5	17.1
0.77% Pt(2.9 nm)/SBA-15	3.1	56	3.9	9.1	49	3.4	19.1
0.6% Pt(3.6 nm)/SBA-15	4.2	31	3.7	9.4	15	1.8	20.9
0.62% Pt(7.1 nm)/SBA-15	9.4	19	4.9	9.8	6	1.6	24.2
Pt(111)[g]	–	–	14.6[h]	8.6	–	15.8[h]	17.9
Pt(100)[g]	–	–	1.3[h]	18.8	–	8.6[h]	22.4
Pt(223)[i]	–	–	7.9[j]	5.0	–	0.4	>8

[a] Particle size determined by counting >200 particles from TEM micrographs

[b] Determined from the total H_2 uptake after O_2 chemisorption (H_2–O_2 titration) and $d(\text{nm}) = 1.13/D$, where D is the dispersion

[c] Standard conditions are 10 Torr C_6H_{10}, 200 Torr H_2, and 313 K (hydrogenation) or 423 K (dehydrogenation)

[d] Normalized by the total number of surface atoms measured by H_2–O_2 titration

[e] Standard conditions were 10 Torr C_6H_{10}, 200 Torr H_2, and 273–323 K for the supported catalysts. The activity in this temperature regime displays 'normal' Arrhenius temperature-dependent behavior

[f] Standard conditions were 10 Torr C_6H_{10}, 200 Torr H_2, and 398–443 K for the supported catalysts. The activity in this temperature regime displays 'normal' Arrhenius temperature-dependent behavior

[g] From reference [8]

[h] The original reaction conditions were 10 Torr C_6H_{10}, 100 Torr H_2, balance He and temperatures specified in (c). The rates were corrected to standard conditions assuming 0.75 order H_2 dependence for hydrogenation [5] and 0.2 reaction order for dehydrogenation (this work)

[i] From reference [7]

[j] The original reaction conditions were 7 Torr C_6H_{10}, 70 Torr H_2, balance He. The rates were corrected to standard conditions assuming 0.75 order H_2 dependence for hydrogenation [5] and 0.2 reaction order for dehydrogenation (this work)

the second desorption state (denoted as β_2) is particle size dependent. The desorption of H_2 ranges from 410 to 440 K on small (~1 nm) particles and 580–600 K for large (5–15 nm) particles; the β_2-hydrogen is most relevant hydrogen species during the hydrogenation of cyclohexene at temperatures greater than the rate maxima. The percentage of total hydrogen desorbed as a β_2 species from a series of silica-supported Pt catalysts (in general) increased with increasing particle size. The increased activity of the Pt(7.1 nm)/SBA-15 for the hydrogenation of cyclohexene at the higher temperatures is supported by fact that the temperature for hydrogen desorption from the β_2 state increases with particle size. The particle-size dependent behavior of H_2 TPD is consistent to explain the particle size dependence of cyclohexene hydrogenation at 448 K: the surface of large particles is covered with adsorbed hydrogen atoms, while 448 K is a temperature greater than the maximum desorption temperature of hydrogen for the small particles (~425 K), resulting in a surface with decreased hydrogen coverage relative to the larger particles (~590 K).

The kinetics for the dehydrogenation of cyclohexene at 423 K are reported in Table 1. The TOF for dehydrogenation varies from ~2 to 9 s^{-1} as the particle size increases from 1.7 to 7.1 nm. The rate of dehydrogenation is more sensitive to particle size than hydrogenation. Over the 'normal' regime of Arrhenius behavior, the apparent activation energy varies from 16 to 24 kcal mol^{-1} (Fig. 1b). At higher temperatures (>550 K), the rate of dehydrogenation leveled off for all particle sizes. In this regime, very small apparent activation energies (~2–3 kcal mol^{-1}) were measured. The decrease in rate is attributed to decrease in cyclohexene and/or H_2 coverage [24, 30]. The dependence of the rate on the pressure of hydrogen is minor, and does not increase significantly with temperature (H_2 reaction order of 0.2 at 413 K compared with 0.3 at 598 K) (see Sect. 3.4).

Table 1 also includes the rates measured for cyclohexene hydrogenation and dehydrogenation at high pressure (760 Torr) on Pt single crystals. It is apparent from Table 1 that the rate of hydrogenation on the single crystal surfaces are on the same order as the Pt/SBA-15 catalyst series, but the rate on Pt(111) is higher than the Pt(100) and Pt(223) surfaces at the reaction conditions (10 Torr C_6H_{10}, 200 Torr H_2, and 313 K) stated in Table 1. The rates of dehydrogenation are again higher on the Pt(111) surface

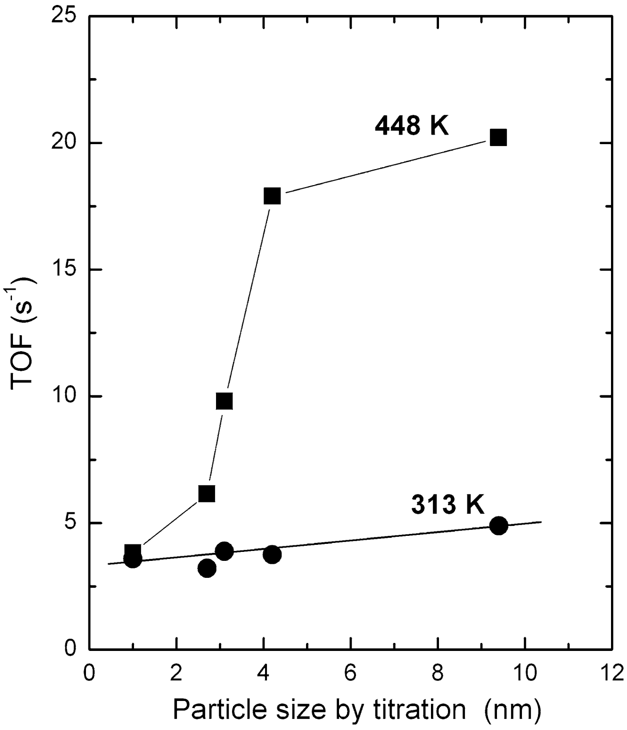

Fig. 2 The influence of particle size on the turnover rate (normalized to the number of surface atoms determined by H_2–O_2 titration) for cyclohexene hydrogenation at two different temperatures (313 and 448 K). The reaction is structure insensitive at low temperatures, and apparently structure sensitive at high temperatures. This difference in reactivity as a function of temperature and particle size is attributed to change in the coverage of *reactive* hydrogen

than the Pt(100) or Pt(223) at the conditions specified in Table 1. The noticeable difference is the rate of dehydrogenation measured on the Pt(223); it is an order of magnitude lower than the Pt(1 nm)/SiO_2 catalyst, which presumably have similar surface structures. An explanation for the structure sensitivity on Pt single crystals has been suggested by McCrea and Somorjai based on characterization of the surface under reaction conditions by sum frequency generation (SFG) surface vibrational spectroscopy [8]. The (100) surface is more active (at temperature of rate maxima) than the (111) surface. A dehydrogenated intermediate, 1,3-CHD has been identified on the Pt(100) surface, while two intermediates (1,3- and 1,4-CHDs) have been identified on the (111) surface by SFG. It is suggested that the 1,3-CHD is the involved in a “fast” reaction pathway for benzene formation and the 1,4 species present only on the (111) surface converts to benzene at a much lower rate because the 1,4-CHD intermediate must initially isomerize to 1,3-CHD before dehydrogenating to benzene. There is no spectroscopic evidence of either species on the surface of NPs and therefore it is inappropriate to suggest the presence of one or both species on the nanoparticle surface during turnover explains the apparent structure sensitivity for benzene hydrogenation.

3.3 Role of Particle Size in Cyclohexene Hydrogenation–Dehydrogenation Selectivity

The dehydrogenation of cyclohexene is more facile on the smaller particles, while hydrogenation is influenced by particle size in a temperature dependent manner (Fig. 2). Figure 3 demonstrates the influence of particle size on the reaction selectivity at 10 Torr C_6H_{10}, 200 Torr H_2 and 423 K. The selectivity to benzene is highest (>60%) on the 1 nm particles and subsequently decreases to less than 10% on large (7.1 nm) particles. This is a unique demonstration of the influence of particle size on reaction selectivity, and these conditions in particular demonstrate the major product can change with particle size. The inset demonstrates that the ability of a particle to change the major product is applicable only under certain experimental conditions. At 523 K, the selectivity to benzene is >60% for all particle sizes, although the selectivity to cyclohexane increases with particle size. The increase in selectivity to cyclohexane at larger particle size is significant and related to an increase in hydrogen coverage (see Sect. 3.4).

The selectivity to hydrogenation–dehydrogenation products during cyclohexene conversion over a wide temperature range is also facet-dependent, as demonstrated by Somorjai and co-workers [8, 30, 31]. On Pt(100) at 423 K, the selectivity to cyclohexane (10 Torr C_6H_{10}, 100 Torr H_2) is 82%, while the corresponding selectivity is 75% on Pt(111). At 523 K, the higher selectivity to the hydrogenation product is now measured on the (111) surface (~34%), while the hydrogenation selectivity on Pt(100) is only ~14% (see Fig. 3 inset). Figure 3 demonstrates that the selectivity for both single crystal matches the 3 nm diameter particle, while the selectivity at 523 K demonstrate the (111) single crystal behaves more like the largest Pt particle, and the Pt(100) continues to behave like the Pt(2.9 nm)/SBA-15 catalyst. The NPs used in this study do not demonstrate well-defined changes in shape with particle size; therefore, we believe the influence of particle size on reaction selectivity is related to changes in the average coordination number of the atoms within the NPs rather than the shape of the nanoparticle.

3.4 Influence of Hydrogen Pressure on Cyclohexene Hydrogenation–Dehydrogenation Activity and Selectivity

The influence of hydrogen partial pressure is shown in Figs. 4 and 5 for the Pt(1 nm)/SiO_2 sample which we believe has the lowest coverage of hydrogen under reaction

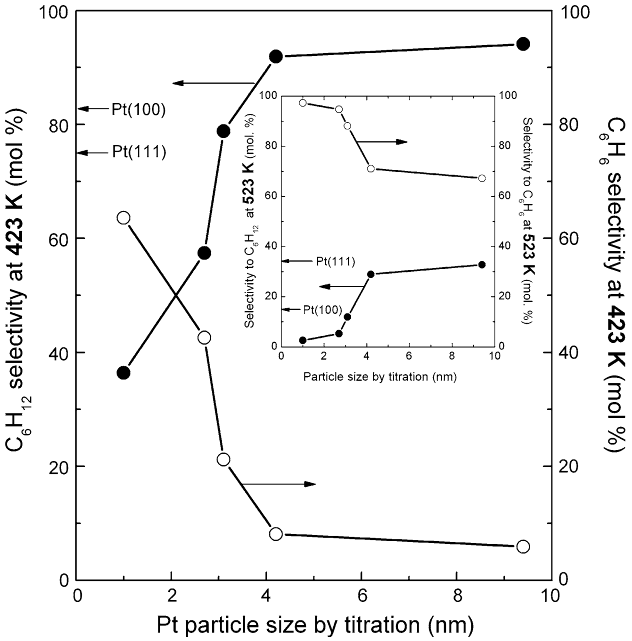

Fig. 3 The influence of particle size on reaction selectivity during the hydrogenation/dehydrogenation of cyclohexene over the series of Pt/SBA-15 catalysts. The reaction conditions are 10 Torr C_6H_{10}, 200 Torr H_2, and 423 K. The inset is the selectivity at 523 K and the same pressure conditions. At 423 K, the particle size dictates selectivity; Pt(1.7 nm) is more selective for the formation of benzene than catalysts with the larger particle size. At higher temperatures, where dehydrogenation dominates, the particle size has a smaller influence on the selectivity to the minor product, cyclohexane. The hydrogenation selectivity is marked on the *ordinate* of the figure (and inset) for Pt(111) and Pt(100) single crystals [8]

conditions.[3] As the pressure of hydrogen increases from 200 to 600 Torr, the dependence of the rate of the hydrogenation reaction changed considerable over a 400 K temperature interval. At low temperatures (303 K), the reaction order in H_2 was 0.48 (see inset of Fig. 4), which is in good agreement with previous measurements on supported Pt catalysts [10] and a Pt powder [5]. As the temperature increased, the reaction order became more positive, and approached values greater than unity. At 548 K, the H_2 reaction order for hydrogenation was ~1.5. A first-order dependence on hydrogen can be derived easily if the addition of a second hydrogen to the half-hydrogenated cyclohexyl (C_6H_{11}) species is rate-determining, but there is no straightforward way based on Langmuir–Hinshelwood kinetic schemes to arrive at a 3/2 order dependence on hydrogen. As the H_2 pressure was doubled from 200 to 400 Torr, there was an increase in the temperature of maximum rate (from ~350 to 373 K). The increase in rate over the entire temperature range suggests that the hydrogen content on the surface increases. Figure 5 demonstrates that the influence of increased hydrogen pressure is less dramatic for the dehydrogenation pathway. At low temperatures (413 K), the pressure dependence on H_2 is 0.2 (inset of Fig. 5). At a temperature of 598 K, the dependence on H_2 does not change substantially. This result is anticipated due to the fact that dehydrogenation only needs hydrogen to remove carbonaceous residues from the surface [23] and the weak dependence on hydrogen may suggest that most of the deposited carbon is mobile enough to migrate to the support without deactivating the catalyst [36]. In temperature-programed reactions (both ascending and descending temperature ramps), we see no indication of high-temperature deactivation.

The increase in H_2 pressure increased the selectivity to cyclohexane over the entire temperature range, but it is most apparent at high temperatures (non-Arrhenius behavior regime) where the steady-state coverage of hydrogen is affected to the greatest extent allowing for

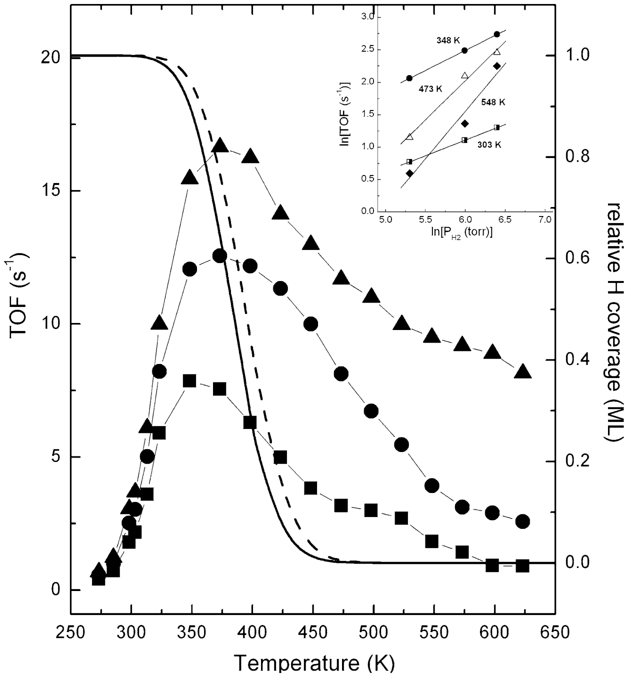

Fig. 4 The influence of H_2 pressure (■) 200 Torr; (●) 400 Torr; and (▲) 600 Torr) on the rate of cyclohexene hydrogenation on the 3.2% Pt(1 nm)/SiO_2 catalysts over the entire temperature range (i.e., normal and non-Arrhenius region). The solid and dashed lines represent the calculation of hydrogen coverage using the initial and monolayer heat of adsorption values [32] in the Temkin isotherm for gas-phase hydrogen pressures of 200 and 600 Torr H_2. The inset demonstrates the change in H_2 reaction order with temperature. At low temperatures (~303 K), the dependence of the reaction rate on the hydrogen pressure is ½ order. The reaction order in H_2 increases as the reaction temperature increases: 0.48 (303 K); 0.61 (348 K); 1.2 (473 K); and 1.47 (548 K)

---

[3] The entire Pt/SBA-15 series demonstrates an increase in rate (and a corresponding change in hydrogenation–dehydrogenation selectivity) with increasing hydrogen pressure. The dependence of the rate of hydrogenation was highly sensitive to the partial pressure of hydrogen over the 400 K interval shown in Fig. 4.

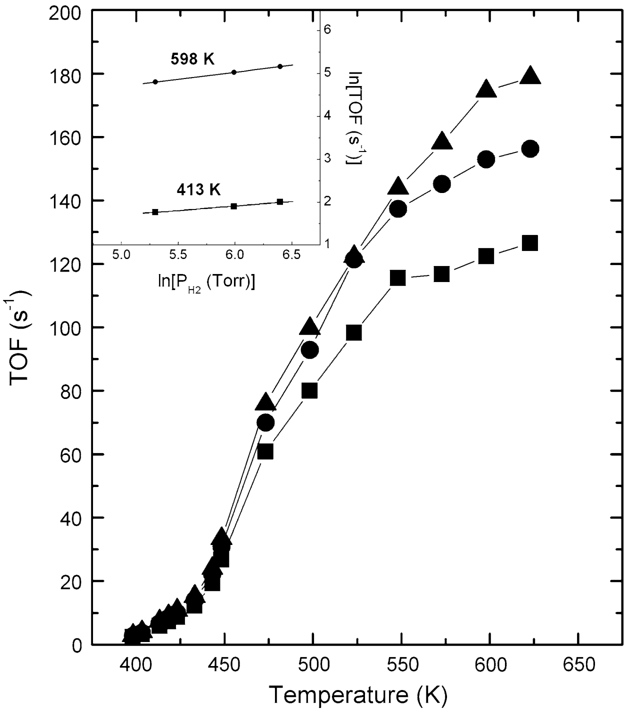

Fig. 5 The influence of H_2 pressure (■) 200 Torr; (●) 400 Torr; and (▲) 600 Torr) on the rate of cyclohexene dehydrogenation on the 3.2% Pt(1 nm)/SiO_2 catalyst over the entire temperature range. The inset demonstrates the change in H_2 reaction order with temperature. At 413 K, the dependence on H_2 is positive but low ($\sim$0.2), and as the temperature increases the dependence on hydrogen increases only slightly (reaction order at 598 K is 0.3)

higher hydrogenation activity. Vannice and co-workers reported the integral heat of adsorption was invariant with particle size for a series of SiO_2-supported Pt catalysts synthesized by standard impregnation methods [32]. An initial heat of adsorption measured on Pt/SiO_2 catalyst with an average particle size of 2 nm was 26.3 kcal mol^{-1} while the room temperature integral heat of adsorption at full monolayer coverage was 24.5 kcal mol^{-1} (these values were used for the Temkin isotherms calculated in Fig. 4 as a function of temperature at two different H_2 partial pressures). TPD studies by Sermon [35] on supported Pt catalysts demonstrate hydrogen requires a range of temperatures to fully desorb (apparent desorption energy, $E_d \geq \Delta H_{ads}$; the apparent activation energy for desorption, $E_{a,d} > 0$) due to the adsorption of different hydrogen populations on energetically non-equivalent sites, suggesting that the two reactions segregate on the surface ([9] and see Appendix I). Although the coverage determined by the Temkin plot calculates zero coverage at temperatures >450 K (Fig. 4), TPD studies demonstrate that hydrogen desorbs at temperatures >600 K, with the larger particles demonstrating more high-temperature hydrogen desorption [35]. We believe that this high-temperature population of adsorbed hydrogen increases with increasing hydrogen pressure (in a particle-size dependent manner) and is responsible for the increased hydrogenation activity with particle size at higher temperatures (Fig. 4).

4 Conclusions

The role of Pt particle size (1.7–7.1 nm) on the *selectivity* to hydrogenation and dehydrogenation products during the conversion of cyclohexene in excess H_2 was examined. The temperature dependence of the reaction is characterized by three regimes: hydrogenation only at low temperature ($\leq$400 K); simultaneous hydrogenation and dehydrogenation at intermediate temperatures ($400 \leq T \leq 550$ K), and predominantly dehydrogenation at high temperatures (>550 K). During simultaneous hydrogenation–dehydrogenation, the rate of hydrogenation decreases with increasing temperature (non-Arrhenius behavior), while benzene formation behaves in a normal Arrhenius manner. At high temperatures, where dehydrogenation dominates, the apparent activation energy remains positive but decreases substantially. The rate of dehydrogenation of cyclohexene to benzene decreases monotonically over the experimental particle size and the apparent activation energy decreases as the metallic dispersion increases. The activity for the hydrogenation of cyclohexene to cyclohexane is structure insensitive under conditions of reversible H_2 adsorption at low temperatures, but becomes structure sensitive at high temperatures due to a particle size dependence on the coverage of reactive hydrogen. The *selectivity* was particle size dependent in the pressure regime studied here (H_2:C_6H_{10} = 20:60) due to a particle-size reactive hydrogen coverage dependence that causes the hydrogenation pathway to become structure sensitive at temperatures where the dehydrogenation of cyclohexene to benzene occurs simultaneously. This work demonstrates that under a particular set of reaction conditions, the selectivity during the conversion of cyclohexene can be influenced by particle size.

Acknowledgments This work was supported by the Director, Office of Science, Office of Advanced Scientific Computing Research, Office of Basic Energy Sciences, Chemical Sciences, Geosciences, and Biosciences Division, of the U.S. Department of Energy under Contract No. DE-AC02-05CH11231. R.M.R. acknowledges the Ford Motor Company for financial support through a graduate fellowship administered by the Berkeley Catalysis Center. The authors acknowledge our long term collaboration with Professor Peidong Yang of the Department of Chemistry at the University of California, Berkeley. The authors would also like to acknowledge Professor M. A. Vannice of the Pennsylvania State University for donation of the 3.2% Pt/SiO_2 material and Dr. Samrat Mukherjee for its preparation.

Appendix I. Deviations from Thermodynamic Selectivity at High Temperatures: Influence of Hydrogen Coverage and Surface Reaction Segregation

The thermodynamics of cyclohexene hydrogenation are favored at low temperatures ($\Delta G_{\mathrm{h}} = -18$ kcal mol^{-1} at 298 K), while the dehydrogenation is favored at high temperatures ($\Delta G_{\mathrm{d}} = -11$ kcal mol^{-1} at 600 K) [37]. The thermodynamic selectivity, defined as $\frac{K_{\mathrm{h}}}{(K_{\mathrm{h}}+K_{\mathrm{d}})}$, where K_{h} and K_{d} are the respective equilibrium constants (and related to the free-energy of reaction, $K = exp\left(\frac{-\Delta G_{\mathrm{hord}}}{\mathrm{RT}}\right)$ for hydrogenation and dehydrogenation is plotted as the *solid line* in Fig. 6. The free-energy reaction data was obtained from [38]. At $400 \leq T \leq 450$ K, the experimentally-measured selectivity for hydrogenation is lower than the thermodynamic selectivity for most samples, although a few of the low-temperature experimentally-measured selectivity data was greater than the thermodynamic value. This is attributed to error in the measurement of the individual reaction rates in this regime where the dehydrogenation activity is low. Figure 6a demonstrates the selectivity for cyclohexane predicted by thermodynamics is much greater than the experimentally-measured values at temperatures >450 K for all catalysts (supported and single crystal). The deviation in this temperature range is related to a much larger decrease in the rate of hydrogenation over this temperature range (see Fig. 1a, the rate of hydrogenation actually decreases with increasing temperature) than the rate of dehydrogenation which has begun to plateau (Fig. 1b). The overall trend of increased hydrogenation selectivity on catalysts containing larger particles is apparent over the entire temperature range as discussed in Sect. 3.2 and demonstrated in Fig. 3. Due to the fact that cyclohexane selectivity is lower than the thermodynamic selectivity, the benzene selectivity will be correspondingly greater than the thermodynamic selectivity (Fig. 6b). For all but a few data points, the selectivity to benzene is greater than that predicted by thermodynamics.

Significant deviations of kinetic selectivity from thermodynamic selectivity has been documented previously for this reaction [9]. The authors suggested that both reactions surface segregate to specific sites on the nanoparticle surface [9]. Cyclohexene dehydrogenates preferentially at low coordination sites (which are more prevalent on smaller particles and consistent with particle-size dependent data (see Table 1)), and the adsorbed hydrogen diffuses away from low coordination sites to higher-coordination sites where it desorbs ($2\mathrm{H}^* \rightleftharpoons \mathrm{H}_2(\mathrm{g}) + 2^*$) immediately or reacts with cyclohexene adsorbed at high coordination sites to form cyclohexane. The hydrogen at the high coordination sites in the presence of adsorbed cyclohexane may

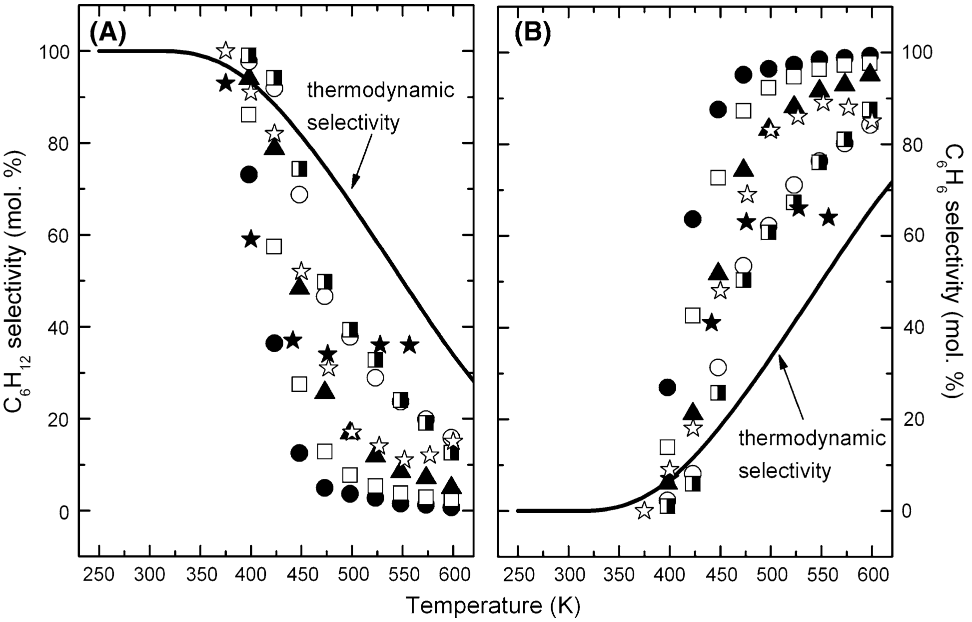

Fig. 6 The selectivity to (**a**) cyclohexane and (**b**) benzene over a number of catalysts: (●) 3.2% Pt(1 nm)/SiO_2; (□) 0.6% Pt(1.7 nm)/SBA-15; (▲) 0.77% Pt/(2.9 nm)/SBA-15; (○) 0.6% Pt(3.6 nm)/SBA-15; and (◨) 0.62% Pt(7.1 nm)/SBA-15, (★) Pt(111) and (☆) Pt(100) single crystal surfaces [8]. The solid line represents the thermodynamic selectivity, based on the temperature dependent Gibbs free-energy ($\Delta G_{\mathrm{rxn}}(T)$) of both hydrogenation and dehydrogenation reactions [38]. The points in (**a**) that lie above the thermodynamic selectivity represent typical uncertainties in the rate measurements, while the points in (**b**) lie above the thermodynamic selectivity line because the decreased hydrogenation rate leads to a selectivity in benzene greater than that predicted by thermodynamics. The reaction conditions were 10 Torr C_6H_{10}, 200 H_2 Torr and the temperature stated on the *x*-axis

represent the high temperature population observed in H_2-TPD studies [35]. The equilibrium occurs in isolation, effectively separating adsorbed hydrogen and hydrocarbon, allowing non-equilibrium yields of benzene. Sermon and co-workers propose that under conditions where both cyclohexene hydrogenation and dehydrogenation occur on the same surface, the two reaction pathways segregate [9]. This picture is consistent with the cyclohexene hydrogenation rate and the observed changes in selectivity with particle size (see Figs. 2 and 3, respectively).

References

1. Che M, Bennett CO (1989) Adv Catal 36:55
2. Boudart M (1969) Adv Catal 20:153
3. Rioux RM, Song H, Hoefelmeyer JD, Yang P, Somorjai GA (2005) J Phys Chem B 109:2192
4. Song H, Rioux RM, Hoefelmeyer JD, Komor R, Niesz K, Grass M, Yang P, Somorjai GA (2006) J Am Chem Soc 128:3027
5. Segal E, Madon RJ, Boudart M (1978) J Catal 52:45
6. Dorling TA, Moss RL (1966) J Catal 5:111
7. Davis SM, Somorjai GA (1980) J Catal 65:78
8. McCrea KR, Somorjai GA (2000) J Mol Catal A Chem 163:43
9. Sermon PA, Georgiades G, Vong MSW, Martin-Luengo MA, Reyes PN (1987) Proc R Soc Lond A 410:353
10. O'Rear DJ, Löffler DG, Boudart M (1985) J Catal 94:225
11. Cogen JM, Ezaz-Nikpay K, Fleming RH, Baumann SM, Maier WF (1987) Angew Chem Int Ed Engl 26:1182
12. Molnár É, Tasi G, Kónya Z, Kiricsi I (2005) Catal Lett 101:159
13. Zaera F (2002) J Phys Chem B 106:4043
14. Mohr C, Hofmeister H, Claus P (2003) J Catal 213:86
15. Mohr C, Hofmeister H, Radnik J, Claus P (2003) J Am Chem Soc 125:1905
16. Vannice MA, Sen B (1989) J Catal 115:65
17. Somorjai GA, Rioux RM (2005) Catal Today 100:201
18. Kim JM, Han YJ, Chmelka BF, Stucky GD (2000) Chem Commun 2437
19. Singh UK, Vannice MA (2000) J Catal 191:165
20. Rioux RM, Komor R, Song H, Hoefelmeyer JD, Grass M, Niesz K, Yang P, Somorjai GA (2008) J Catal 254:1
21. Deitz WA (1967) J Gas Chromatogr 5:68
22. Fási A, Pálinkó I, Katona T, Bartók M (1997) J Catal 167:215
23. Paál Z (1985) J Catal 91:181
24. Yoon KJ, Vannice MA (1983) J Catal 82:457
25. Orozco JM, Webb G (1983) Appl Catal 6:67
26. Wootsch A, Paál Z (1999) J Catal 185:192
27. Wootsch A, Paál Z (2002) J Catal 205:86
28. Bond GC, Slaa JC (1994) Catal Lett 23:293
29. Bond GC, Slaa JC (1995) J Mol Catal A Chem 98:81
30. Yang M, Rioux RM, Somorjai GA (2006) J Catal 237:255
31. Bratlie KM, Flores LD, Somorjai GA (2005) Surf Sci 599:93
32. Sen B, Vannice MA (1991) J Catal 130:9
33. McCabe RW, Schmidt LD (1976) Surf Sci 60:85
34. McCabe RW, Schmidt LD (1977) Surf Sci 65:189
35. Vong MSW, Sermon PA (1987) J Chem Soc Faraday Trans 83:1369
36. Parera JM, Figoli NS, Traffano EM, Beltramini JN, Martinelli EE (1983) Appl Catal 5:33
37. Vong MSW, Sermon PA (1987) J Chem Soc Faraday Trans 83:1667
38. Janz GJ (1954) J Chem Phys 22:751